

# Estimation of transducer translation using channel-domain correlation

Nick Bottenus

Department of Biomedical Engineering, Duke University, Durham, NC

Corresponding author email: nick.bottenus@duke.edu

**Abstract**—Swept synthetic aperture imaging has been previously proposed as a method of extending the effective size of an ultrasound transducer to improve lateral resolution, especially at depth. This method requires precise knowledge of array position and orientation in space as it is moved across a field of view. Previous experimental realizations have used motorized translation stages or calibrated measurement arms to track the transducer. We demonstrate a 1 degree-of-freedom sweep device that constrains the transducer motion and enables a new channel-domain motion estimation method. This channel correlation method is compared against conventional speckle tracking motion estimation and the known applied motion from a motorized stage. Swept synthetic aperture was successfully performed in a phantom using both estimators without external position tracking to extend a 2 cm transducer over a 5 cm sweep and achieve a lateral resolution improvement of 70%.

**Index Terms**—transducer motion, speckle tracking, channel correlation, high resolution, large aperture

## I. INTRODUCTION

Ultrasound array extent is directly related to lateral image resolution – larger arrays make higher resolution images with a limit approaching the axial resolution. While axial resolution is reasonably constant with imaging depth, lateral resolution degrades linearly with depth. A large aperture size combined with an aperture growth strategy that maintains a fixed ratio of imaging depth to aperture size can combat this effect to produce images with more constant lateral resolution throughout. Large arrays may be useful in improving image quality for deep targets such as in abdominal imaging, even in the presence of acoustic clutter [1]. However, larger footprint arrays require more individual transmit and receive channels and scanner electronics, adding both cost and complexity and limiting their clinical utility.

We have previously proposed a technique for overcoming these trade-offs by using transducer motion to form effectively larger arrays, or a “swept synthetic aperture” (SSA) [2]. Pulse-echo data from multiple transducer positions are coherently combined using precisely known position and orientation of the array relative to the target or a global frame of reference. Unlike extended field-of-view techniques [3], this synthetic aperture method effectively extends the array and produces higher lateral resolution. The requirement for position tracking has limited past realizations of the device to translation stages

This work was funded by NIH R01-EB017711 from the National Institute of Biomedical Imaging and Bioengineering and R01-CA211602 from the National Cancer Institute.

that apply a motorized displacement or calibrated mechanical arms that measure and calculate the end effector position, neither of which is ideal for clinical imaging. We seek a solution that removes the bulky, expensive fixture and allows the sonographer freedom to perform high-resolution imaging on-demand with minimal disruption of their current workflow.

Instead of an external position tracking device, we demonstrate a fixture that simply constrains the transducer motion to one degree-of-freedom – lateral translation within the imaging plane. Conventional lateral speckle tracking techniques are used to estimate the motion with sufficient accuracy to form SSA images. We also introduce a new aperture-domain tracking technique that estimates transducer motion directly using channel data rather than relying on beamformed images. This reduces computational complexity and directly estimates in the domain of motion rather than limiting the estimate to a selected lateral region.

## II. METHODS

### A. 1-D constrained sweep

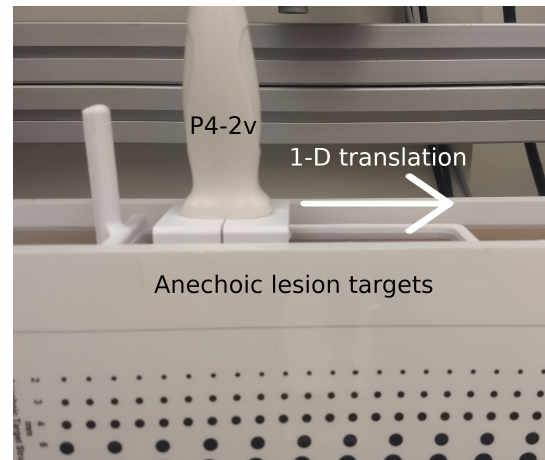


Fig. 1. Constrained 1-D sweep device. The P4-2v transducer is placed into a molded sled, which slides on a 1-D plastic track in the lateral direction within the imaging plane while an interleaved transmission sequence is acquired.

Two sets of swept aperture experimental data were collected. In both cases the Verasonics Vantage 256 ultrasound scanner (Verasonics, Inc., Redmond, WA) was used with the P4-2v phased array transducer to acquire receive channel data from a sequence of transmissions. An interleaved transmission

sequence was designed to transmit a plane wave followed by a virtual source diverging wave from both ends of the array in succession. An ATS 549 tissue mimicking phantom (CIRS, Norfolk, VA) was imaged with anechoic lesion targets and point targets in a homogeneous speckle-generating background. Data were stored for offline processing.

First, data with a known motion profile were collected using a Newport XPS-Q8 motion controller (Newport, Irvine, CA, USA) and a Newport UTM100 linear translation stages (5-m on-axis accuracy and 1.5-m uni-directional repeatability). The stage was swept in 1500 steps over 50 mm laterally and synchronized with the Verasonics acquisition such that repeated transmissions (e.g. plane wave to plane wave) were spaced 0.1 mm apart.

Second, experimental data were collected using a constrained motion device to allow manual control of the transducer (i.e. moving at an unknown, time-varying rate) along a prescribed 1-D path of approximately 5 cm. This device is shown in Fig. 1. Motion of the transducer was limited to the lateral direction of the imaging plane, matching the direction of the lateral array elements. The extent and temporal profile of this motion were unknown. The three interleaved transmissions were repeated at 500 Hz for 1 second total.

### B. Speckle tracking

Lateral speckle tracking [4] for estimation of transducer motion was performed using the acquired data from plane wave transmissions. Images were formed using plane wave beamforming and envelope detection for each acquired frame. Lateral pixel size was chosen to be slightly smaller than the element pitch, 0.2 mm, to reduce computational cost of the correlation while maintaining high quality estimates. To estimate the displacement between two images, a 1 cm x 1 cm kernel was selected at 2 cm depth from the reference frame and compared to laterally shifted kernels, up to 2.5 mm in single pixel increments, from the target frame using normalized cross correlation. The resulting correlation curve was upsampled using spline interpolation to select the shift location of peak correlation. The result of this process for a sample pair of images is shown in Fig. 2.

### C. Channel correlation

Channel correlation was performed similarly to lateral speckle tracking except in the aperture domain rather than the image domain. No beamforming was performed for this method. To estimate the displacement between two channel data sets, a 1 cm axial kernel was selected at 2 cm depth from both the reference and target frames. Normalized cross correlation of the channel data was performed with zero padding, up to 10 elements of displacement (approximately 2.5 mm). A nonlinear interpolation function based on quadratic subsample estimation was used to find the shift location of peak correlation while reducing estimate bias due to element pitch. The result of this process compared to speckle tracking is shown in Fig. 2.

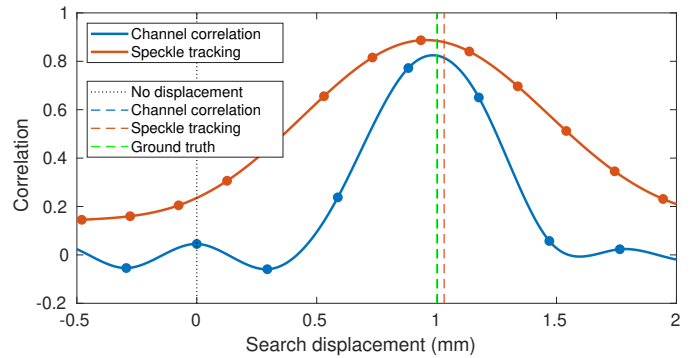


Fig. 2. Method of subsample estimation for an example pair of data frames. Channel correlation is performed by interpolation of correlations between element groups. Speckle tracking is performed by peak estimation of lateral overlapping kernel estimates.

### D. Multi-lag estimation

More robust displacement estimates were obtained in both cases by combining estimates from multiple pairs of frames using weighted least squares estimation, with correlation values as weights. Estimates from up to 10 frames prior to each given frame were included to solve for a consistent solution across the entire sequence.

### E. Swept synthetic aperture beamforming

Swept synthetic aperture beamforming was performed for the experimental data by beamforming each diverging wave frame given the estimated position of the transducer from above. Focusing delays were calculated relative to a common output image grid. Focused data were coherently combined with a Tukey weighting across the swept aperture extent to increase the contribution of low lateral spatial frequencies and restore a conventional point spread function (PSF) shape.

## III. RESULTS

The applied motion of the translation stage was used as the ground truth for SSA imaging. Fig. 3 shows the imaging results of an individual transmission (plane wave and diverging) as well as the coherently combined SSA result using each type of transmission. The plane wave demonstrated a limited field of view compared to the diverging transmission (the image was masked based on assumed beam profile) but is expected to remain highly correlated over small translations due to the near-constant transmit geometry. However, the limited footprint of the plane wave restricts the coherent combination over multiple transducer positions, resulting in only slight improvement in SSA lateral resolution. The diverging wave overlaps deep targets from a much wider set of transducer positions, resulting in a large synthetic aperture and high lateral resolution.

A reference image is shown from the P4-2v used in a conventional imaging mode in Fig. 4. This represents the maximum resolution achievable from the 2 cm aperture. Both speckle tracking and channel correlation were applied to the translation stage data set and their estimates were used

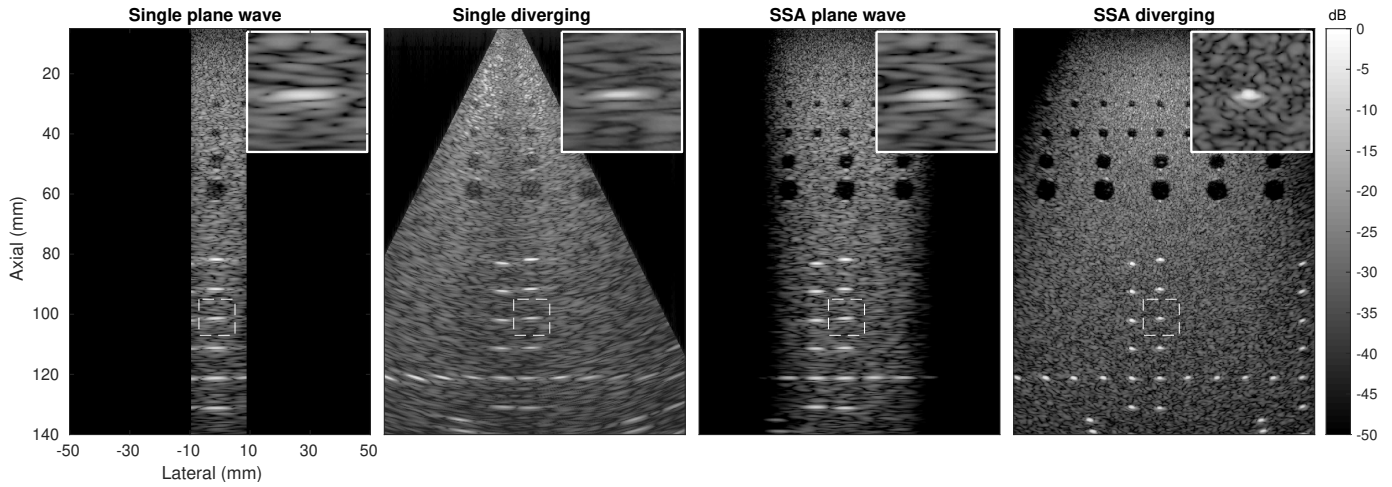


Fig. 3. Experimental phantom images using the motorized translation stage to move the P4-2v transducer and known applied displacements to register image frames. (left to right) Single plane wave transmission, single diverging wave transmission, SSA image formed with plane waves, SSA image formed with diverging waves. Diverging waves provide maximum spatial overlap and the largest effective aperture size.

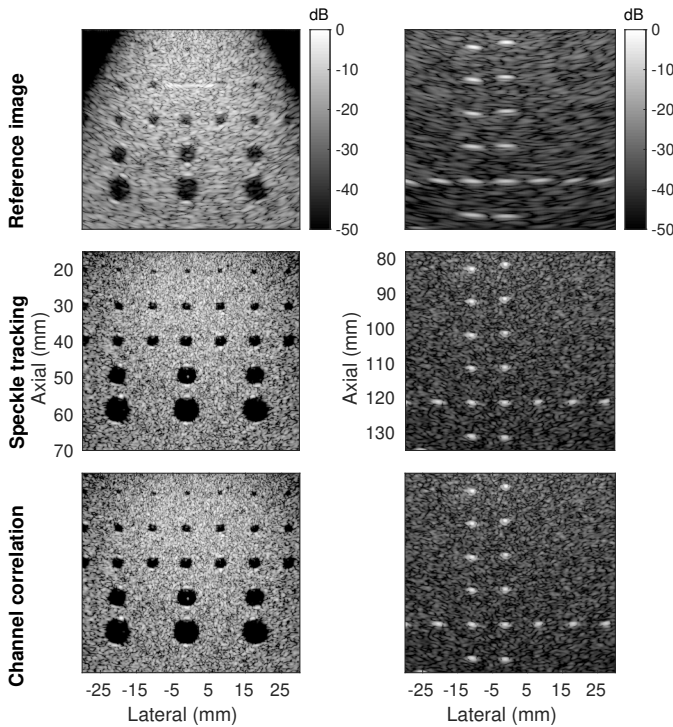


Fig. 4. (top) Reference image from the P4-2v, a 2 cm aperture. (middle, bottom) SSA images formed with motion estimates using lateral speckle tracking and channel correlation respectively over a 5 cm sweep. Lesion and point targets are shown from the larger field of view of Fig. 3.

in place of the known applied transducer position for SSA beamforming. The estimates in both cases were sufficient to produce a higher resolution image with finer speckle texture, improved edge resolution, and a narrower lateral PSF as shown in the images of Fig. 4.

The point target at 100 mm depth represents a deep imaging target that is poorly resolved by the small phased array

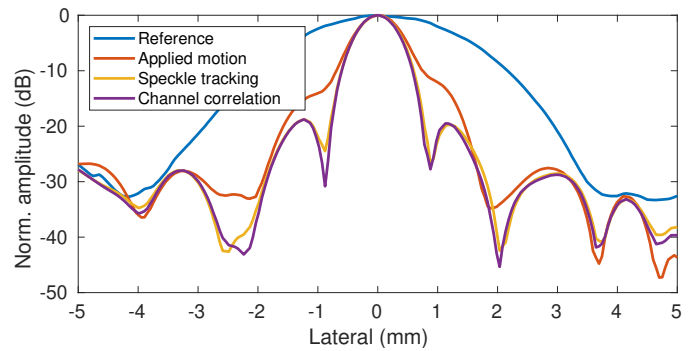


Fig. 5. Lateral point spread functions for target at 100 mm depth from reference frame and SSA images with known and estimated motion.

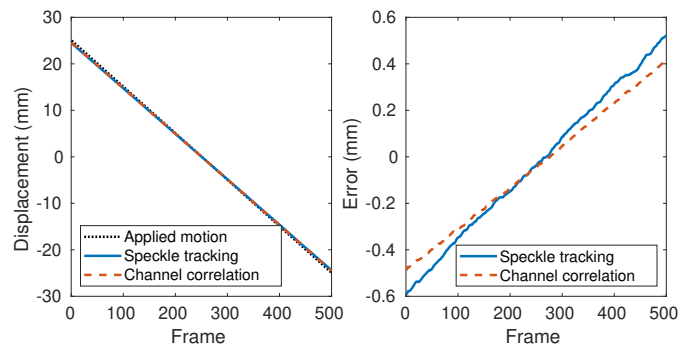


Fig. 6. (left) Actual and estimated displacement across the 50 mm sweep. (right) Error in estimate relative to the applied motion at each frame.

transducer with a full-width at half-maximum (FWHM) of 3.22 mm. After SSA imaging with a 5 cm sweep, point target resolution was improved to 1.01, 0.96, and 0.91 mm for the applied displacement, speckle tracking estimate, and channel correlation estimate respectively. The PSFs are shown in Fig. 5. We believe that the estimation methods produced better resolution than the ground truth due to slight misalignment

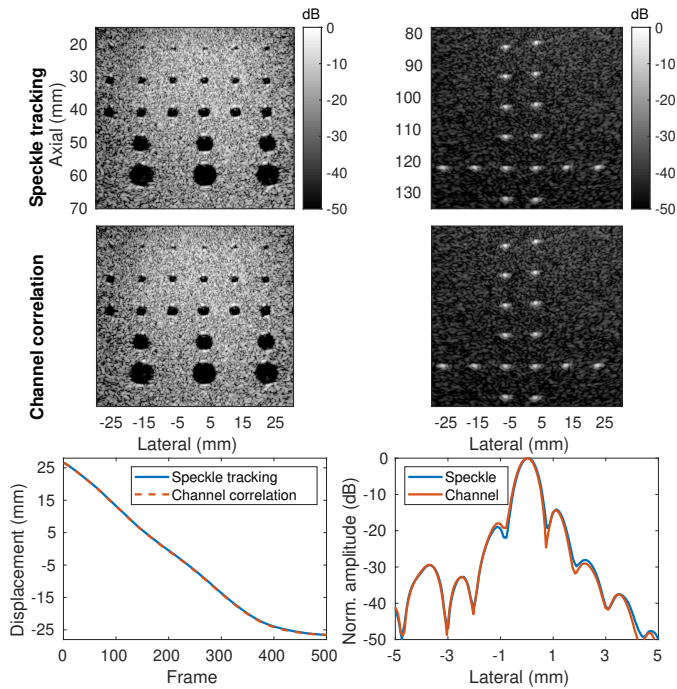


Fig. 7. SSA results from manual sweep using constrained motion device. Note that transducer position and motion do not match the translation stage case. Lateral point spread functions for target at 100 depth.

between the lateral translation stage and the imaging plane which the estimators can account for. The estimates are shown in Fig. 6 along with the error relative to the applied displacements. Note that the estimates show low frame-to-frame jitter as required for SSA imaging, while the bias in the estimates likely accounts for the previously mentioned misalignment.

Fig. 7 shows the SSA imaging results, estimated displacements, and PSFs for both estimation methods when using the manual constrained motion device rather than the translation stage. The applied motion profile is not perfectly linear in this case, showing acceleration of the transducer throughout the sweep. Both estimators produced similar estimates and resulted in a FWHM of 0.85 mm for the point target near 100 mm depth.

#### IV. DISCUSSION

The two estimators were both observed to perform well for tracking 1-D motion of the transducer when constrained to the lateral dimension. However, we expect there to be differences in performance between the estimators to be studied in future work.

The computational complexity of the channel correlation method is slightly less than that of speckle tracking. Channel correlation does not require a separate image focusing and beamformation step and seems to perform well with fewer lateral dimension samples (64 channels compared to 100 pixels for these experiments). This difference increases drastically with larger lateral kernels for speckle tracking.

Channel correlation suffers from lower correlation values than speckle tracking due to the lack of beamformer gain, which is expected to worsen jitter of the estimates [5]. However, especially for targets near the transducer, channel correlation should be higher using a nearly constant plane wave transmission and subset of receive elements compared to beamformed image data. The channel correlation method should also be more robust to speed of sound errors and aberration, but may be more sensitive to reverberation and incoherent noise.

The data-based estimators were robust to misalignment of the motion plane relative to the image plane. Both methods would suffer in the presence of target motion, although an additional axial correlation step may be able to compensate for the motion. These methods could trivially be extended to matrix arrays and 2-D motion, where the computational efficiency of the channel correlation method would be even more advantageous.

The required sampling rate of the scanner is dependent on the speed of motion and the uncertainty of the estimators as a function of distance. Large displacements result in decorrelation and therefore increased estimate jitter, while fast sampling increases the computational complexity of motion estimation. An adaptive processing scheme to balance these two effects would be useful for processing SSA data.

#### V. CONCLUSIONS

We have demonstrated swept synthetic aperture imaging for high lateral resolution without external motion tracking. The ultrasound echo data was used in the channel and image domains to perform lateral motion estimates of the transducer with sufficient accuracy for coherent combination of the data.

#### ACKNOWLEDGMENT

The author would like to thank Gregg Trahey for feedback in preparation of this work. The author would also like to thank Easha Kuber for scanning and modeling the P4-2v for the slide device and Vaibhav Kakkad for preliminary work on speckle tracking.

#### REFERENCES

- [1] N. Bottenus, W. Long, M. Morgan, and G. Trahey, "Evaluation of Large-Aperture Imaging Through the ex Vivo Human Abdominal Wall," *Ultrasound in Medicine & Biology*, vol. 44, no. 3, pp. 687–701, 2018.
- [2] N. Bottenus, W. Long, H. K. Zhang, M. Jakovljevic, D. P. Bradway, E. M. Boctor, and G. E. Trahey, "Feasibility of Swept Synthetic Aperture Ultrasound Imaging," *IEEE Transactions on Medical Imaging*, vol. 35, no. 7, pp. 1676–1685, 2016.
- [3] L. Weng, A. Tirumalai, and C. Lowery, "US extended-field-of-view imaging technology," *Radiology*, vol. 203, no. 3, pp. 877–880, 1997.
- [4] G. E. Trahey, J. W. Allison, and O. T. von Ramm, "Angle independent ultrasonic detection of blood flow," *IEEE transactions on bio-medical engineering*, vol. 34, pp. 965–7, dec 1987.
- [5] W. F. Walker and G. E. Trahey, "Fundamental limit on delay estimation using partially correlated speckle signals," *IEEE Transactions on Ultrasonics, Ferroelectrics, and Frequency Control*, vol. 42, no. 2, pp. 301–308, 1995.